Supplementary Material (ESI) for Polymer Chemistry

SUPPORTING INFORMATIONS

S1. The water uptake was evaluated from difference in weight before and after complete dryness of the membranes for the determination of volume fraction of water in the membrane matrix. Membrane was immersed in distilled water for 24 h and its wet weight was recorded after complete removal of surface water by absorbing paper. Weight of dry membrane (W_d) was recorded for dried membrane sample (under vacuum at 60 °C for 10 h) until a constant weight is obtained. The thickness of wet and dry membranes was determined by using a digital micrometer up to an accuracy of 0.1μm. The volume fraction of water in the membrane matrix (φ_w) of the membranes was determined by following equation:

$$water\ uptake\ (\varphi_w, \%) = \frac{W_{wet} - W_{dry}}{W_{dry}} \times 100 \qquad (1)$$

where W_{wet} and W_{dry} are the weight of the membrane under wet and dry conditions. The ion exchange capacity of the membranes was determined using the Mohr method, in which the membranes in the chloride form were converted into the sulfate form via immersing in aqueous Na_2SO_4 solution (0.5 M) for 8 h. The chloride ions released from the membranes were titrated with aqueous $AgNO_3$ solution (0.10 m). The IEC values were calculated from the released chloride ions and expressed as mequiv.g^{-1} of dry membrane (Cl^- form).

S2. Experimental cell used for the determination of transport number had two asymmetric compartments separated by a circular piece of membrane (7.0 cm^2) and electrodes. The cathodic and compartment capacity was 200 ml and 20 ml. The electrodes, obtained from Titanium Tantalum Products (TITAN, Chennai, India) were made of expanded TiO_2 sheet coated with a triple precious metal oxide (titanium–ruthenium–platinum) (6μm thickness), with 1.5mm thickness and 25.0 cm^2 area. Distance between both electrodes and the effective membrane area was 0.11 cm and 25.0 cm^2, respectively. Peristaltic pumps were used to feed NaCl solution (0.1M) in a recirculation mode into the cathodic compartments while distilled water into the anodic compartment with constant flow rate. In order to control both the current intensity and the voltage, digital multimeter was

placed in series to apply the current across the electrodes. The applied current density was 8 $mAcm^{-2}$. Experiments were carried out for 1 h and samples were taken out from the anodic and cathodic compartments and determine the Cl^- ion concentration. The counter ion transport number (Cl^-) was determined by

$$t_-^m = \frac{nF}{It}\left(C^- V^- - C^0 V^0\right) \qquad (2)$$

where n is the charge on chloride ion (Cl^-), F is the Faraday constant, I is the applied current, t is the time. C^0 and C^- are the initial and final concentration of Cl^- in the anodic compartment while, V^0 and V^- are the initial and final volume of anodic compartment. Membrane permselectivity was estimated from counter-ion transport number in the membrane phase obtained from Hittorf method.

Table S1: Physico-and electro-chemical properties of the used cation-exchange membrane (CEM) in ED experiment

Properties	CEM
Thickness (μm)[1]	150
Water content (%)[2]	13.6
Ion-exchange capacity (mequiv./ g of dry membrane)[3]	0.93
Counter -ion transport number (t_i^m)[a, 4]	0.95
Specific membrane conductivity (S cm^{-1}) [b,5]	2.02×10^{-2}

[a] *measured by membrane potential in equilibration in with 0.01 M and 0.1 M NaCl solutions.*
[b] *measured in equilibration with 0.1 M NaCl solution.*
Uncertainty for measurements: 1: 1.0 μm; 2: 0.1%; 3: 0.01 mequiv./g of dry membrane; 4: 0.01; and 5: 0.01× 10^{-3} S cm^{-1}.

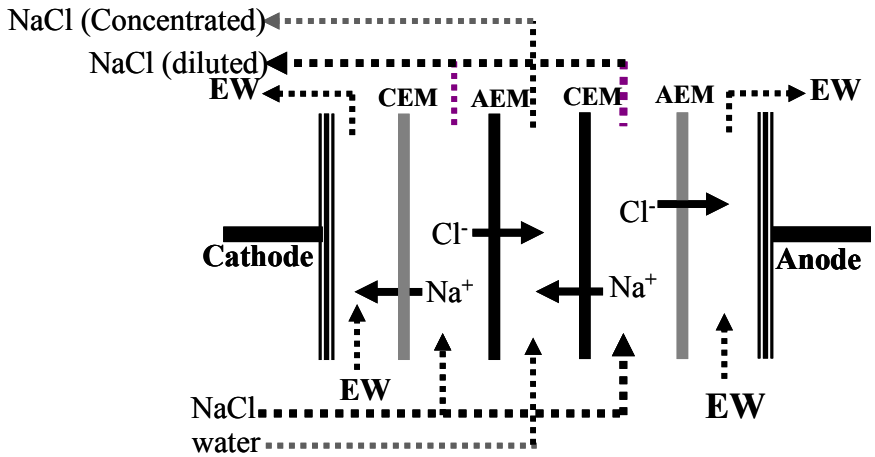

Fig. S1 Schematic diagram of ED cell for salt separation.

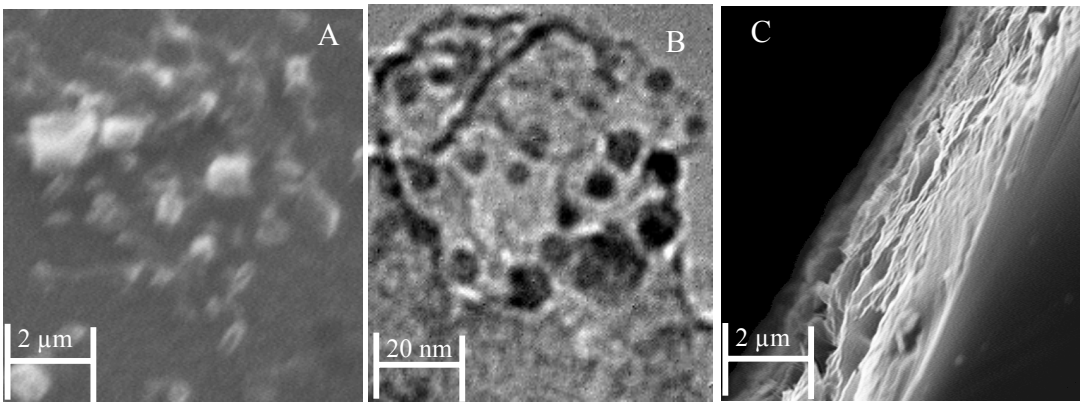

Fig. S2 SEM and TEM images of hybrid AEM-70.

Table S2 Oxidative and hydrolytic loss in weight, ion-exchange capacity (IEC), and membrane conductivity (κ^m) for developed AEMs.

Membrane	Oxidative stability (loss %)			Hydrolytic stability (loss %)		
	Weight	IEC	κ^m	Weight	IEC	κ^m
AEM-50	2.6	5.65	2.35	7.81	7.34	3.35
AEM-60	2.0	8.82	2.56	8.61	10.44	4.56
AEM-70	1.6	9.42	2.89	10.47	11.59	4.89

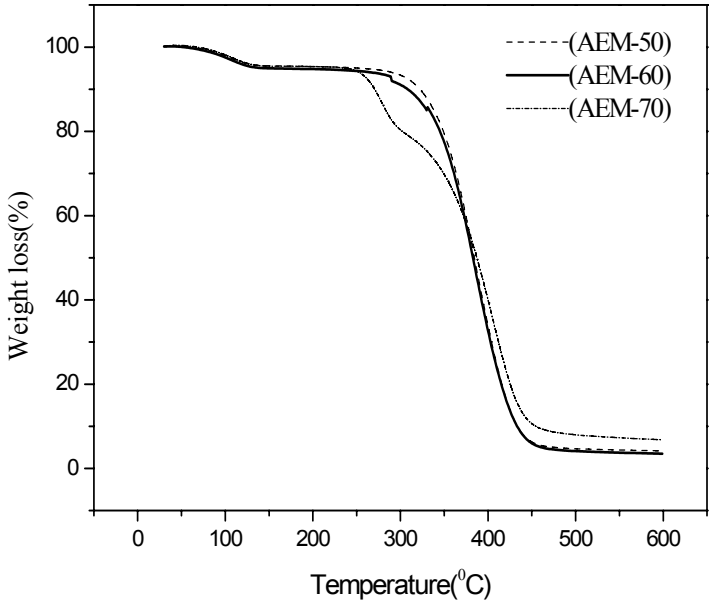

Fig. S3 TGA curves for AEMs with varied amount of AESP.

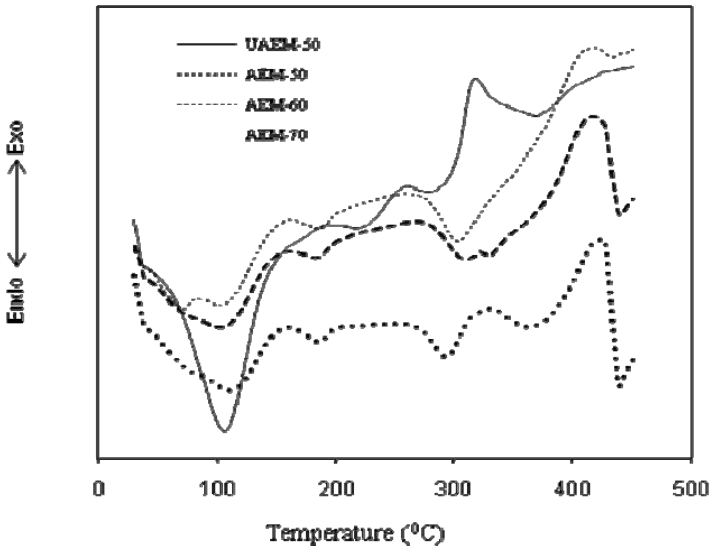

Fig. S4 DSC thermograms for AEMs with varied amount of AESP in completely dried state.

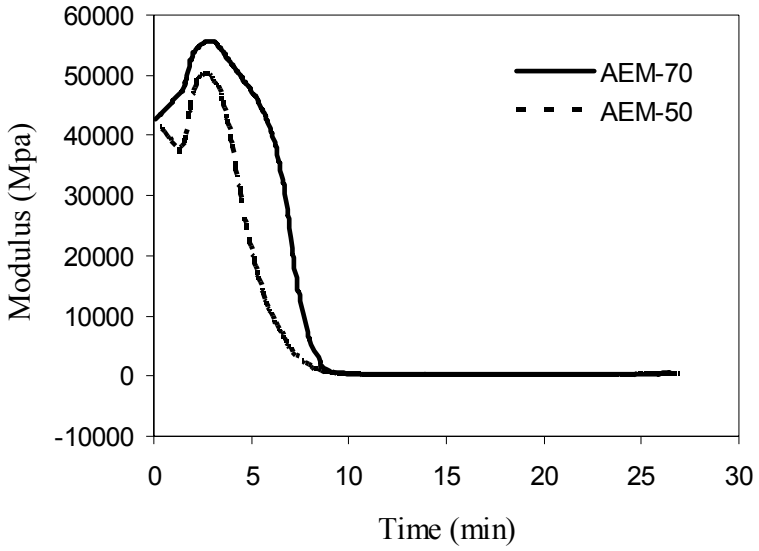

Fig. S5 Dynamic mechanical analysis curves for hybrid AEMs with varied AESP content.

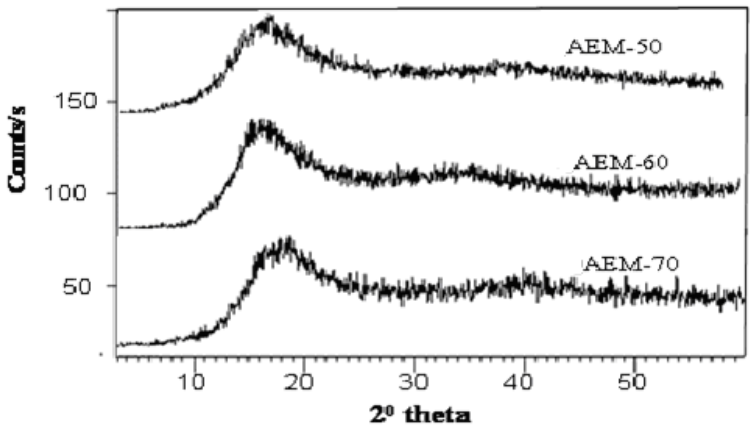

Fig. S6 WXRD patterns of the hybrid AEMs with varied AESP content.

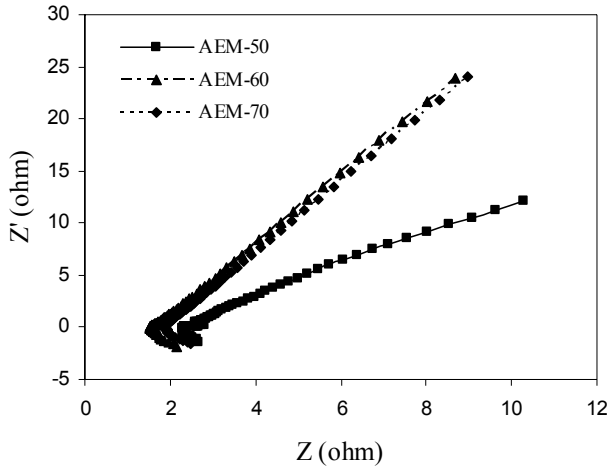

Fig. S7 Nyquist plots for hybrid AEMs with different AESP content in equilibration with NaCl solution (0.1M).

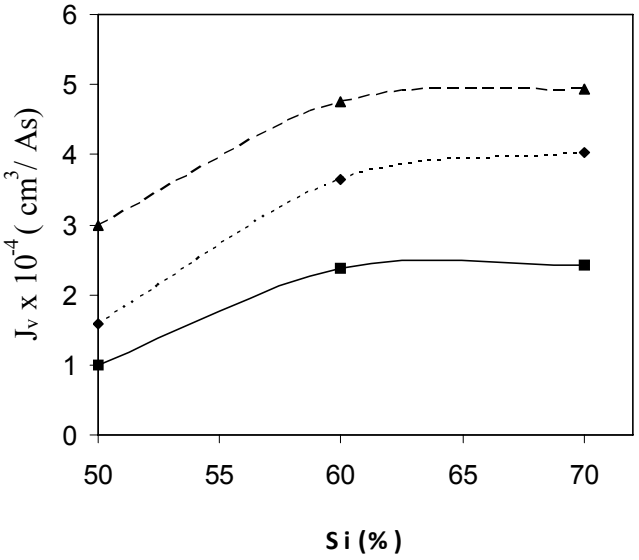

Fig. S8 Variation in electro-osmotic flux with AESP content of hybrid AEMs.

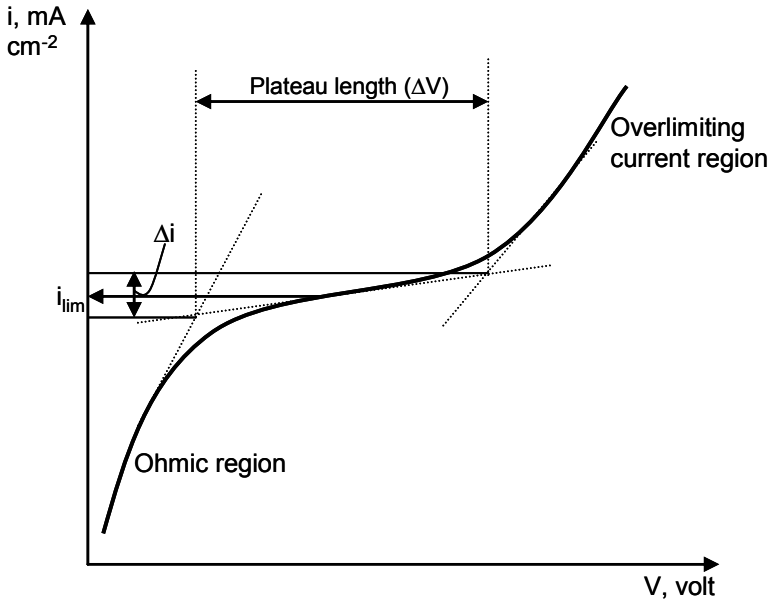

Fig. S9 Schematic presentation of *i-v* curve for the hybrid AEM.

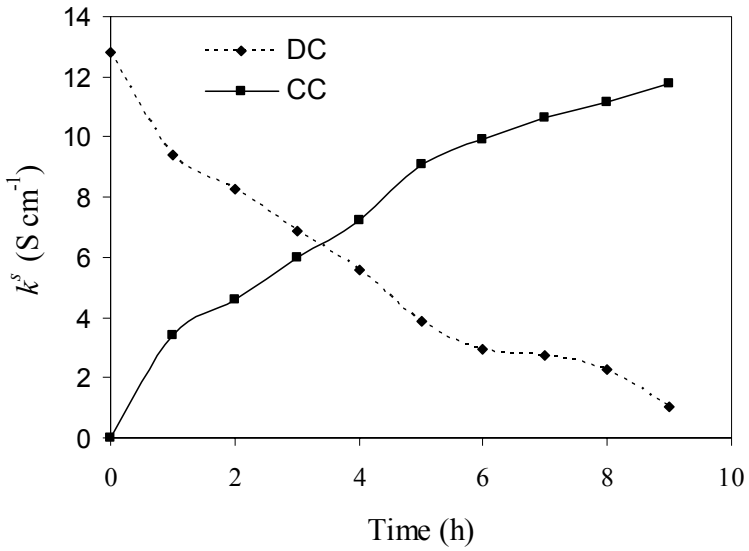

Fig. S10 Variation in solution conductivity for DC and CC for hybrid AEM-70: DC feed - 0.2M NaCl solution at 4.0V applied potential.

S3. The ED process performance was evaluated in terms of rate of salt (NaCl) removal (*J*), current efficiency (*CE*) and energy consumption (*W*: kWh/kg of NaCl removed). Considering negligible mass flow through membranes, J may be obtained by following equation:[2,3]

$$J = \frac{V_a}{A}\frac{C_t - C_0}{\Delta t} \qquad (3)$$

where C_0 and C_t are the initial and final concentration of NaCl in CC (mol m^{-3}), Δt the time (s) allowed for ED, V_a the total volume of CC feed (0.50×10^{-3} m^3), and A is the effective membrane area (8.0×10^{-3} m^2). Rate of salt migration (*J*) across developed AEMs are presented in Fig. 1 as a function of time. In beginning, salt migration increased with time under constant applied voltage and attained maxima. Further it was decreased because of progressively lowered NaCl concentration in DC. Different AEMs followed the trend: AEM-70>AEM-60>AEM-50 for rate of salt migration, similar to their conductivity, charge concentration or permselectivity.

W and *CE*, defined as the fraction of Coulombs utilized for the salt removal, of the ED process were obtained by following equations:[2]

$$W\left(kWhkg^{-1}\right) = \int_0^t \frac{VI\,dt}{m} \qquad (4)$$

where *V* is the applied voltage, *I* the current, *t* the time allowed for the electrochemical process, and *m* is the weight of salt removed.

$$CE(\%) = \frac{m\,n\,F}{M\,Q} \times 100 \qquad (5)$$

where *F* is the Faraday constant, *M* the molecular weight of salt, *n* the stoichiometric number (*n* = 1 in this case), and *Q* is the electric quantity passed (Coulombs; *A s*). To evaluate the electrodialytic performance of developed AEMs, energy consumption and

CE (%) data, obtained under similar experimental conditions, are presented in Table 5. It was observed that *W* decreased, while CE increased with AESP content in the membrane matrix. We also observed that the content of AESP in the membrane matrix leads the availability of ionic groups in the membrane matrix, which was responsible for high membrane permselectivity, conductivity, and fixed charge concentration along with low electro-osmotic drag of mass (solvent) across the membrane, which are the essential electro-chemical properties for an efficient AEM. These parameters (*W* & *CE*) also depends on the operating conditions of an ED unit. Under optimum operating conditions (after the passage of 10.2 $\times 10^3$ Coulombs electricity), for AEM-70 membrane, *CE* and *W* were found to be 86.7% and 11.2 kWh kg^{-1}, respectively, which showed potential of developed AEM for electrochemical processes.